Design and Evaluation of Finger-operated Teleimpedance Interface Enabling Simultaneous Control of 3D Aspects of Stiffness Ellipsoid

Kraakman, F.M.C.; Peternel, L.

DOI
10.1109/Humanoids58906.2024.10769954

Publication date
2024

Document Version
Final published version

Published in
Proceedings of the IEEE-RAS 23rd International Conference on Humanoid Robots (Humanoids)

Citation (APA)
Kraakman, F. M. C., & Peternel, L. (2024). Design and Evaluation of Finger-operated Teleimpedance Interface Enabling Simultaneous Control of 3D Aspects of Stiffness Ellipsoid. In *Proceedings of the IEEE-RAS 23rd International Conference on Humanoid Robots (Humanoids)* (pp. 690-697). (IEEE-RAS International Conference on Humanoid Robots). IEEE. https://doi.org/10.1109/Humanoids58906.2024.10769954

2024 IEEE-RAS 23rd International Conference on Humanoid Robots (Humanoids)
Nancy, France. November 22-24, 2024

2024 IEEE-RAS 23rd International Conference on Humanoid Robots (Humanoids) | 979-8-3503-7357-8/24/$31.00 ©2024 IEEE | DOI: 10.1109/Humanoids58906.2024.10769954

Design and Evaluation of Finger-operated Teleimpedance Interface Enabling Simultaneous Control of 3D Aspects of Stiffness Ellipsoid

Frank M.C. Kraakman, and Luka Peternel

***Abstract*— In this paper, we present a design and evaluation of a novel finger-operated teleimpedance interface used to command stiffness ellipsoids to the remote robot. The proposed interface provides a practical alternative to the state-of-the-art teleimpedance interfaces based on physiological signals that can be impractical in daily use. On the other hand, as opposed to existing practical interfaces that lack in terms of controlled degrees of freedom, the proposed interface enables control of 3D aspects of the ellipsoid. The remote robot stiffness ellipsoid is controlled with a single hand using the thumb, index, and middle fingers to operate two scroll wheels, a joystick, and a force sensor. These combinations of inputs can be mapped to control different aspects of the stiffness ellipsoid, i.e., orientation and shape/size. To investigate different modes of input mapping, we perform a human factors experiment to evaluate the performance and user acceptance of the proposed interface modes. The results of the experiments indicate that the participants can successfully operate the interface to complete 3D stiffness configuration alignment tasks in different modes. To further demonstrate the functionality of the proposed teleimpedance interface, we performed an additional experiment utilising a Force Dimension Sigma7 haptic device to control the motion of a KUKA LBR iiwa robotic arm while performing a complex physical interaction task.**

I. Introduction

As humanoid robots are getting increasingly integrated into our daily lives there is a growing need for them to perform physical interaction tasks. When humans work with robots in close proximity they can physically interact with them directly to collaborate on and teach them how to perform various tasks. However, when humanoid robots are sent to perform tasks at remote sites such as inspection & maintenance, and disaster response, humans can only influence robots remotely [1], [2].

The concept of teleoperation enables humans to control and teach remote robots at a distance [3]. Often remote robots have to operate in unstructured and unpredictable environments where control of physical interaction is crucial to successful task execution [4]. It has been shown that humans deal with such cases by modulating the mechanical impedance of the limbs to achieve a proper relationship between force and motion for a given task [5]. Similarly, variable impedance control can be used on robots to improve their physical interaction capabilities [6]. A method in teleoperation that enables human operators to control the impedance of the remote robot in real-time is called teleimpedance [7]. The key component in this approach is the teleimpedance interface with which the human operator can adjust the stiffness of the robot limbs.

Authors are with Cognitive Robotics, Delft University of Technology, 2628 CD Delft, The Netherlands (e-mail: l.peternel@tudelft.nl).

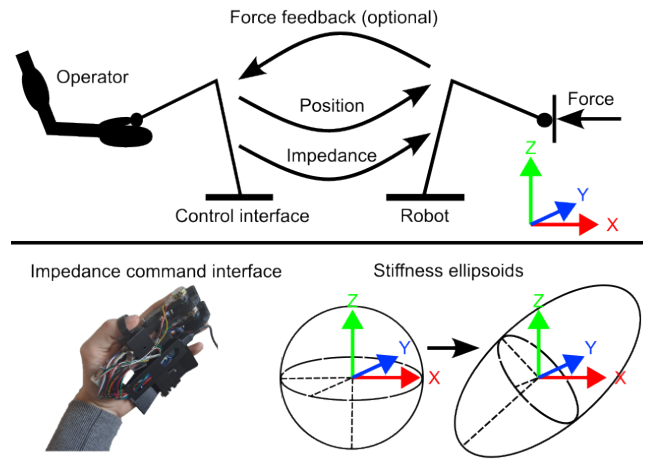

Fig. 1: Conceptual illustration of a teleoperation system (top) and the novel teleimpedance interface that adjusts the stiffness ellipsoid configuration (bottom).

In literature, there are several types of teleimpedance interfaces (i.e., stiffness command interfaces) that enable the operator to control the remote robot stiffness. One of the most common is based on measuring the operator's arm impedance via electromyography (EMG) and then mapping it to the robotic arm impedance [8]–[13]. The key advantage of these interfaces is their intuitiveness as the operator can simply stiffen or relax their arms to give commands. However, the drawback is the complexity associated with the use of EMG where equipping and calibration procedures may affect the applicability and robustness. Furthermore, if used in bilateral teleoperation, there is a coupling effect between force feedback and stiffness commands, which can take away some of the operator's control due to involuntary reflexes [14]. Alternatively, approximate muscle activity can be potentially estimated using computer vision [15], nevertheless, such an approach requires an external camera with an unobstructed view of the human operator's arm.

More practical alternative interfaces are based on measuring hand grip with a force sensor [16], buttons/sliders [17]–[19], and foot-based rotating plate [20]. At the expense of some intuitiveness, these interfaces considerably reduce the complexity compared to EMG and do not have the coupling effect between force feedback and commanded stiffness. Nevertheless, the control inputs are typically limited in terms of degrees of freedom (DoF), thus the operator cannot control all aspects of the stiffness ellipsoid simultaneously and independently (orientation, shape, and size).

Other interfaces based on wiggling of haptic interface

[21] or inducing perturbations at haptic interface [22] enable multi-DoF control of stiffness ellipsoid. However, they induce interruptions to the operator position commands, which can degrade task performance. A touchscreen interface based on creating and adjusting virtual ellipsoids with fingers [23] enables simultaneous and independent control of all aspects of stiffness ellipsoids without perturbing position commands. However, this interface takes considerable visual and cognitive attention from the operator, as the operator has to look at the touchscreen when forming virtual ellipsoids.

Therefore, the existing impedance command interfaces have various limitations in terms of setup complexity, limited degrees of freedom, interruptions, and dividing the operator's attention. The objective of this study is to develop a novel hand-held interface that would retain the main advantages and overcome the main limitations. Based on this we set the following design requirements for the new interface:

- R1: The use of interface does not involve complex equipping and calibration procedures or knowledge of human anatomy.
- R2: Aspects of 3D stiffness ellipsoid can be commanded simultaneously (orientation, shape, and size).
- R3: Does not introduce a coupling effect between force feedback and the commanded stiffness.
- R4: Does not require the operator to look at the interface during operation.

Using these requirements as a guideline, we designed a novel hand-held interface operated by three fingers (see Fig. 1 for illustration). The thumb operates a joystick, while the index and middle fingers operate two scroll wheels. Such a design avoids biosignals (e.g., EMG), and thus does not require complex equipping or calibration procedures (R1) and there is no coupling effect (R3). Since the operator relies on proprioceptive feedback on fingers, he/she does not need to look at the interface while controlling joystick/scroll-wheel inputs (R4). The control input options can be allocated to change different aspects of the stiffness ellipsoid (orientation, shape, and size) simultaneously (R2). In this study, we explored two main modes of control input allocation, wherein in one mode the joystick was assigned to control shape/size and the scroll wheels to control orientation, while in the other mode, the allocation was reversed. To validate the proposed interface and compare the main modes, we first conducted a human factors experiment. Finally, we conducted demonstration experiments with the better-performing mode to showcase the interface in a complex teleoperated physical interaction task.

II. Methods

The block diagram in Fig. 1 illustrates the key components of a teleimpedance system that utilises the novel stiffness command interface. This system consists of two locations: the local site, where the operator generates the real-time motion and impedance commands, and the remote site, where the remote robot receives the commands and executes the task. At the local site, a haptic device measures the operator's movements and uses them as commanded reference positions for the remote robot. The haptic device can optionally also provide feedback about the forces experienced by the remote robot to the operator. The hand-held teleimpedance interface is controlled by fingers to create stiffness ellipsoids that are commanded to the remote robot.

A. Preliminaries for the design

Some design assumptions were made for the interface design. For this study, we are focused on translation stiffness, thus the rotational stiffness was fixed. For tasks in a 3D environment, translational stiffness configuration can be represented as a 3D ellipsoid with shape/size and orientation. We need six variables to fully define a 3D stiffness ellipsoid in terms of shape/size and orientation. The six variables consist of the lengths of the three principal vectors for the shape/size of the ellipsoid and three angles for the orientation around its centre point.

The actual sizes and ratios between the principal vectors depend on the task and its requirements. Most of the tasks require ellipsoids that are either shaped as a sphere, prolate (one longer principal axis compared to the other two), or oblate (one shorter principal axis compared to the other two). A spherical shape would be used in tasks where equally high or low stiffness is needed in all directions, such as in the case of general point-to-point movements. Examples of common tasks where a non-spherical shape is needed are the peg-in-the-hole task and a surface polishing task. The peg-in-the-hole task is a prime example where a prolate-shaped stiffness ellipsoid (Fig. 1, right-bottom) would be used, where the elongated/stiff part of the ellipsoid is aligned with the hole to have pushing power. At the same time, the two narrow/compliant parts are aligned with the surface plane so that the peg can easily slide along the plane into the hole. The surface polishing task is a prime example of where an oblate-shaped stiffness ellipsoid (shaped like a disk) would be used, where the narrow/compliant part would be aligned perpendicularly to the surface to ensure any rough/variable sections on the surface do not produce excessive forces. At the same time, the two elongated/stiff parts are parallel with the surface plane so that the robot can achieve accurate trajectory tracking on the surface despite the friction. Since prolate and oblate shapes are sufficient in most common tasks, we can make an assumption that two principal vectors have the same length. This reduces the number of required configuration inputs from six to five.

For many tasks, just changing the shape/size of the stiffness ellipsoid is not enough. In these cases, we must also orient the ellipsoid to align with the task objective. When the stiffness ellipsoid is rotated, this is done around the x-, y-, and z-axis of the base frame of the stiffness ellipsoid (typically the same as the robot base frame). Assuming prolate and oblate shapes, to orient the stiffness ellipsoid in any orientation we need only 2 rotations about different axes. This is because the third rotation (i.e., around the longer principal axis for prolate shapes or around the shorter

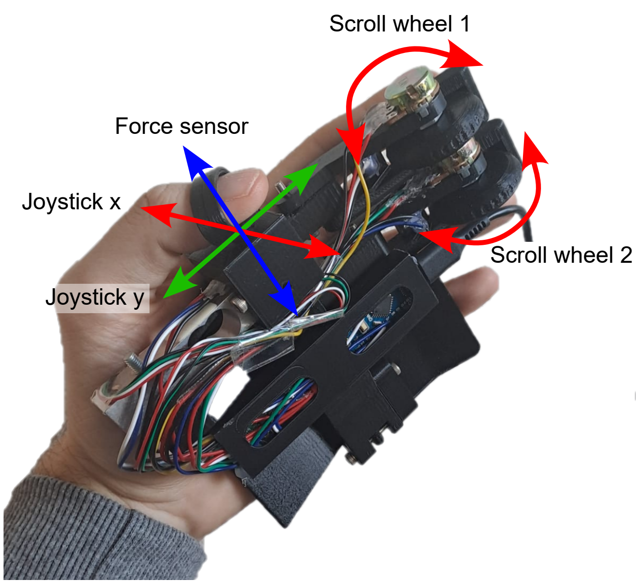

Fig. 2: Closer look at the designed finger-operated teleimpedance interface. The input sensors' locations and actuation directions are indicated by arrows. The input functionalities for the two main modes are described in Tab. I.

principal axis for oblate shapes) does not affect the ellipsoid configuration, as the other two principal axes have the same lengths. Thus, one rotational direction can be omitted. With this final simplification, the number of variables required to be configured with the stiffness command interface can be reduced from five to four. The four variables remaining are two lengths of the principal vectors and their orientations.

B. Teleimpedance interface design

1) Implementation Details: With the preliminary analysis and assumptions made in Section II-A, it was determined that to control four variables, the stiffness command interface needs at least four inputs. To obtain these main four inputs, we employed two scroll wheels (two 0th-order control inputs) and one 2D joystick (two 1st-order control inputs). With the 0th-order input, the operator has direct control over the value where the set value is mapped directly and remains constant over time (e.g., computer mouse). The 1st-order input involves the operator controlling the amount of change per time step rather than having direct control over the values themselves (e.g., joystick or steering wheel).

We chose the scroll wheels and a joystick for their familiarity as they are often used in everyday devices like computer mice and gaming consoles. We also integrated a force sensor into the joystick, acting perpendicular to the joystick's plane of movement, which adds two more 1st-order control inputs (i.e., pull and push). Furthermore, two click buttons were positioned adjacent to the scroll wheels that can be used to alter the mode of operation or be reprogrammed for alternative functions.

Figure 2 shows the designed stiffness command interface with the control inputs. Two scroll wheels, linked to rotational potentiometers, were placed along the index and middle fingers. These wheels were arranged similarly to those found on a standard computer mouse, with an

TABLE I: Input allocations for Modes 1 and Mode 2 of the proposed teleimpedance interface. Angles θ and ϕ define the rotations, while s_1 and s_3 define the lengths of independent principal axes of prolate/oblate ellipsoids, while s_2 is dependent. Size scales independent lengths proportionally.

Input	Scr. wheel 1	Scr. wheel 2	Joystick	Force sensor
Finger	Index	Middle	Thumb	Thumb
Control	0th order	0th order	1st order	1st order
Mode 1	θ	ϕ	s_1 and s_3	Size
Mode 2	s_1	s_3	θ and ϕ	Size

adjustable distance to the palm to accommodate operators with different hand sizes. A joystick was mounted on top of a force sensor, which was located close to the thumb's resting position. This allows the operator to move the joystick in a plane (left-right, forward-backward). We added a ring on the joystick that encloses the operator's thumb. This improves stability for movement in the plane, as well as enables the thumb to also pull on the force sensor besides pushing.

There are many possible combinations of which of the inputs control which aspects of the ellipsoids with the designed interface. In this study, we focused on two main modes given in Tab. I. In Mode 1, scroll wheels control the orientation of the ellipsoid, while the joystick controls the shape/size. In Mode 2, scroll wheels control the shape/size of the ellipsoid, while the joystick controls the orientation. In both modes, we use the additional inputs from the force sensor to provide some redundancy to the control of ellipsoid size. Pushing on the button increases the stiffness ellipsoid size while pulling decreases the overall size of the stiffness ellipsoid. We did not deploy force sensor input for the main four variables since it requires more effort than scroll wheels or a joystick, due to force input rather than position. Since the joystick and force sensor are 1st-order control inputs, there is a change in the controlled variable unless the input is perfectly zero, which can produce undesirable changes in practice. Hence, we implemented a small dead zone to remove undesired drifts.

2) Technical Specifications: The frame of the interface, joystick ring and base, scroll wheels, and click buttons were all custom 3D-printed from PLA plastic. The joystick was based on a generic 2D joystick from game controllers. We extended it by integrating a 2-kg load cell with SparkFun HX711 24-bit amplifier to also measure the push/pull actions of the thumb. To measure the angle of the wheels, 1 kΩ resistance potentiometers were used. The click bottoms were two frames/arms enclosing the scroll wheels. We used Arduino Nano with a 10-bit AD converter to process signals from the joystick, rotational potentiometers, and click buttons.

C. Remote robot impedance controller

To control the translational stiffness of the remote robot $\boldsymbol{K}_t \in \mathbb{R}^{3\times3}$, we need to transform the inputs from the stiffness command interface into the stiffness matrix. We construct it by using the lengths of the principal axes as eigenvalues of this matrix, and the rotation angles as eigenvectors. The constructed matrix is defined as

$$\boldsymbol{K}_t = \boldsymbol{R}\boldsymbol{U}\boldsymbol{S}\boldsymbol{R}^T, \tag{1}$$

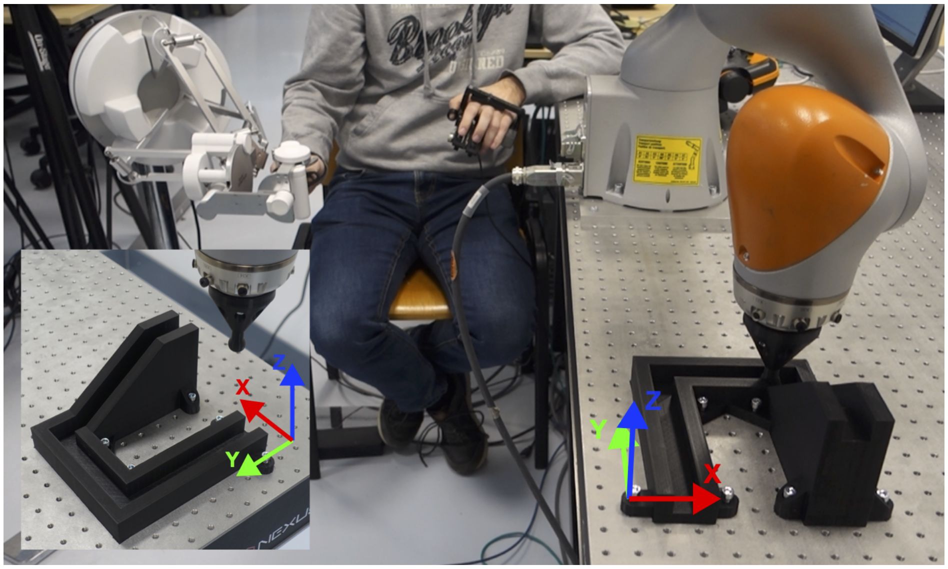

Fig. 3: Illustration of experimental setup. The developed teleimpedance interface is held in the operator's left hand, while the Force Dimension Sigma7 haptic device is held in the right hand. These two command stiffness and motion, respectively, of the remote KUKA LBR iiwa7 robotic arm to perform the task of physically navigating the u-shaped slot mounted to the table. The orientation of the reference frame is indicated by red, green, and blue arrows.

where $\boldsymbol{U} \in \mathbb{R}^{3\times3}$ is a diagonal matrix containing unit conversion factors from internal interface units into stiffness units. $\boldsymbol{S} \in \mathbb{R}^{3\times3}$ is a diagonal matrix that contains the eigenvalues related to the lengths of the principal axes of the ellipsoid and is defined as

$$\boldsymbol{S} = \begin{bmatrix} s_1 & 0 & 0 \\ 0 & s_2 & 0 \\ 0 & 0 & s_3 \end{bmatrix}. \tag{2}$$

In Mode 1, lengths s_1 and s_2 are configured by moving the joystick left-right, and s_3 by moving the joystick forward-backward. In Mode 2, s_1 and s_2 are adjusted using the scroll wheel at the index finger, and s_3 is adjusted using the scroll wheel at the middle finger (see Tab. I). The eigenvector matrix is obtained from a rotation matrix $\boldsymbol{R} \in \mathbb{R}^{3\times3}$, which is defined by inputs that control θ and ϕ as

$$\boldsymbol{R} = \begin{bmatrix} \cos(\theta) & -\sin(\theta)\cos(\phi) & \sin(\theta)\sin(\phi) \\ \sin(\theta) & \cos(\theta)\cos(\phi) & -\cos(\theta)\sin(\phi) \\ 0 & \sin(\phi) & \cos(\phi) \end{bmatrix} \tag{3}$$

In Mode 1, angles θ and ϕ are controlled by the scroll wheels, while in Mode 2 they are controlled by the joystick (see Tab. I).

The full robot stiffness matrix $\boldsymbol{K} \in \mathbb{R}^{6\times6}$ is composed of both translational stiffness $\boldsymbol{K}_t$ form (1) and rotational stiffness $\boldsymbol{K}_r \in \mathbb{R}^{3\times3}$ as

$$\boldsymbol{K} = \begin{bmatrix} \boldsymbol{K}_t & 0 \\ 0 & \boldsymbol{K}_r \end{bmatrix} \tag{4}$$

Rotational stiffness matrix $\boldsymbol{K}_r$ is constructed using the eigenvectors obtained from $\boldsymbol{K}_t$ as

$$\boldsymbol{K}_r = \boldsymbol{R}\boldsymbol{\Sigma}\boldsymbol{R}^T, \tag{5}$$

where $\boldsymbol{\Sigma} \in \mathbb{R}^{3\times3}$ is a diagonal matrix containing predefined rotational stiffness values. In this study, we used a rotational stiffness of 50 Nm/rad for all three axes.

Stiffness matrix $\boldsymbol{K}$ is then used to control the remote robot end-effector force by the impedance controller as

$$\boldsymbol{F} = \boldsymbol{K}(\boldsymbol{x}_d - \boldsymbol{x}_a) + \boldsymbol{D}(\dot{\boldsymbol{x}}_d - \dot{\boldsymbol{x}}_a), \tag{6}$$

where $\boldsymbol{x}_a$ represents the actual pose, $\boldsymbol{x}_d$ signifies the reference pose of the robot end-effector, while $\boldsymbol{K} \in \mathbb{R}^{6\times6}$ and $\boldsymbol{D} \in \mathbb{R}^{6\times6}$ denote the virtual Cartesian stiffness and damping matrices, respectively. The stiffness matrix is adjustable with the novel stiffness command interface. The damping matrix is dependent on stiffness and is obtained by the double diagonalization design [24].

The endpoint force was controlled at the robot joint-torque level while accounting for the dynamics of the robot as

$$\boldsymbol{M}(\boldsymbol{q})\ddot{\boldsymbol{q}} + \boldsymbol{C}(\boldsymbol{q},\dot{\boldsymbol{q}})\dot{\boldsymbol{q}} + \boldsymbol{g}(\boldsymbol{q}) + \boldsymbol{J}^T(\boldsymbol{q})\boldsymbol{F} = \boldsymbol{\tau}, \tag{7}$$

where $\boldsymbol{F}$ represents the interaction force/torque exerted by the robot on the environment and consists of interaction forces from the task $\boldsymbol{F}_{task}$ and force from the impedance controller $\boldsymbol{F}_{imp}$, $\boldsymbol{q}$ denotes joint angles, $\boldsymbol{\tau}$ corresponds to joint torques, $\boldsymbol{J}$ is the robot Jacobian matrix, $\boldsymbol{M}$ is the mass matrix, $\boldsymbol{C}$ is the centrifugal and Coriolis matrix, and $\boldsymbol{g}$ is the gravity vector.

III. Experiments

Fifteen participants between the ages of 20 and 57 years (Mean = 28.8±9.9) took part in the experiment: four females and eleven males. The interface design and experiment protocols were approved by the TU Delft Human Research Ethics Committee. All participants gave written informed consent prior to their participation. The experimental work was divided into two experiments. The goal of the first experiment was to conduct a human factors study to evaluate the designed interface and modes in terms of performance and usability for ellipsoid creation. The experimental conditions were the two modes defined in Sec. II-B. The goal of the

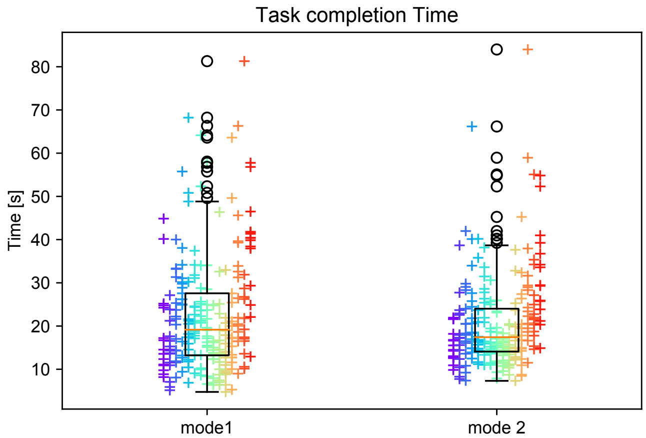

Fig. 4: Results on time it took participants to complete full adjustment of the stiffness ellipsoid (i.e., orientation and shape/size). The y-axis represents task completion time, and the x-axis denotes the mode of the teleimpedance interface. The red horizontal line indicates the median time among participants, the box highlights the interquartile range, whiskers denote the maximum and minimum values, and circles denote outliers. Individual + marks indicate values for individual trials, while different colors indicate individual participants.

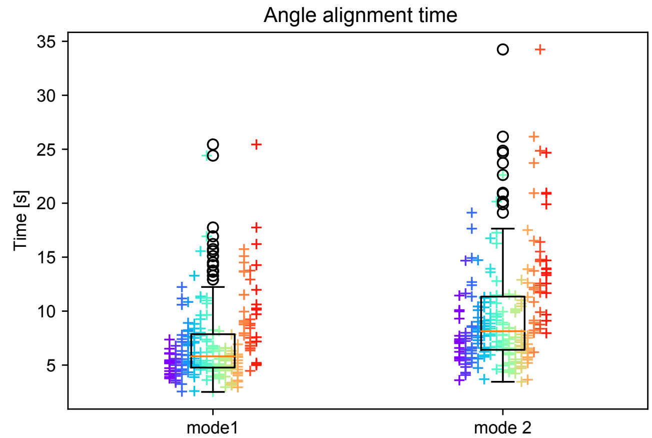

Fig. 5: Results on time it took participants to adjust the orientation of the stiffness ellipsoid.

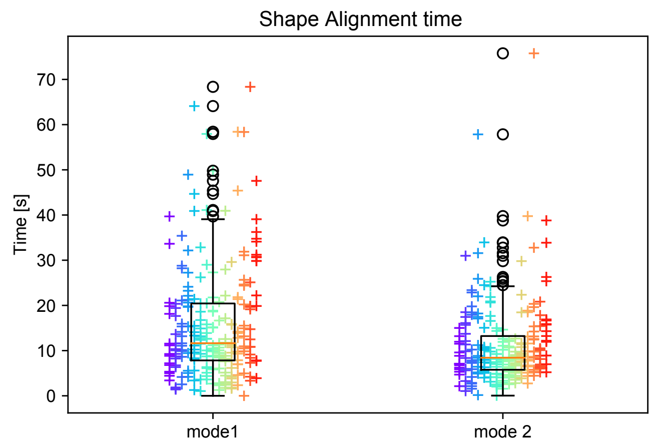

Fig. 6: Results on time it took participants to adjust the shape/size of the stiffness ellipsoid.

second experiment was to leverage the results of the first experiment in selecting the better mode and then perform a demonstration of the teleimpedance system on a complex physical interaction task (see Fig. 3).

A. *Experiment 1: Human Factors Study*

Before the first experiment, the participants were introduced to the concept of teleimpedance and then familiarised with the experiment and the interface. During the first experiment, the participants were presented with a task where they had to align the commanded ellipsoid to different target reference ellipsoids. They were instructed to first align the orientation and then shape/size, which was found to be the most effective strategy in the pilot study. This enabled us to measure and analyse the times for each sub-task also separately. The 3D ellipsoids were displayed in real-time on a computer screen where the screen was split in two to show the view in two planes. The alignment was considered successful when the commanded ellipsoid matched within 5% of the reference ellipsoid in orientation and shape/size (i.e., ϕ, θ, s_1, s_3). At that point, a new reference ellipsoid was presented and the completion time was recorded. The recorded completion times contain two separate values: the time to align both angles with the reference and the time to complete the whole alignment. Each full alignment to the reference ellipsoid was considered one trial and orientations and shape/size of ellipsoids varied between the trials.

To reduce the learning effect, the experimental conditions (i.e., interface Mode 1 and Mode 2) were presented to the participants in an alternating manner: the odd-numbered participants began in Mode 1, while the even-numbered participant numbers began with Mode 2. For both conditions, the experiment has three blocks. The first two blocks were used for training to further reduce the learning effect. Each of the training blocks was limited to 5 minutes and a maximum of 30 trials (i.e., reference ellipsoids). The third block was used to collect the data for the analysis, where the participant performed 15 trials (i.e., 15 reference ellipsoids) with no time constraints. Thus, completion times are the objective metric of the first experiment.

After completing blocks for both conditions, the participant was also asked to fill out a custom Likert questionnaire and the standard van der Laan questionnaire [25] for both Mode 1 and Mode 2. These questionnaires provided subjective metrics of the first experiment to give insight into usability. The Likert questionnaire consisted of the following statements:

- S1: ”The Shape/size of the ellipsoid was easier to manipulate with the joystick in comparison to the scroll wheel”.
- S2: ”The orientation of the ellipsoid was easier to manipulate with the joystick in comparison to the scroll wheel”.
- S3: ”The mental workload was higher for Mode 1 in comparison to Mode 2”.
- S4: ”The physical workload was higher for Mode 1 in comparison to Mode 2”.

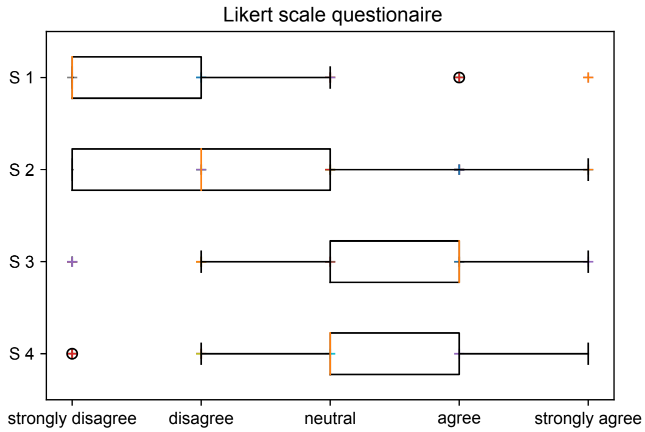

Fig. 7: Results of the Likert questionnaire regarding participants' preferences between the two interface modes. S1 and S2 relate to whether the participants preferred the joystick over the scroll wheels to adjust orientation and shape/size. S3 and S4 relate to participants' experience of mental and physical workload.

The participants had to indicate to what extent they agreed on the scale: strongly agree, agree, neutral, disagree, and strongly disagree.

Using the Shapiro test, the obtained data was first tested to check whether it was normally distributed. If data was normally distributed, a t-test could be used to check the significance of the difference between the completion times of different modes. For the data that were not normally distributed, we used the Wilcoxon signed-rank test. Fig. 4 shows the overall results for the total task completion times, which include both alignments of stiffness ellipsoid orientation and shape/size. The median time to complete the entire alignment task was 22.53$\pm$13.32s for Mode 1 and 20.51$\pm$10.51s for Mode 2. However, the difference was statistically not significant (p=0.30).

To gain a deeper insight, we also investigated completion tasks for orientation and shape/size sub-tasks. Figure 5 shows the results of completion times for orientation alignment. The median time it took the participants to align the angles was 6.85$\pm$3.38s for Mode 1 and 9.44$\pm$4.58s for Mode 2. The difference was statistically significant ($p = 0.0033$). Figure 6 shows the results of completion times for shape/size alignment. The median time it took the participants to adjust the shape/size to the correct size was 15.68$\pm$12.44s for Mode 1 and 11.07$\pm$8.96s for Mode 2. The difference was statistically significant ($p = 0.0011$).

The results of the Likert questionnaire are illustrated in Fig. 7, where the red vertical lines indicate median values of the agreement to each statement. Most participants found the scroll wheel easier to use for adjusting the shape/size of the stiffness ellipsoids compared to a joystick, thus they generally did not agree with S1. The scroll wheel was also preferred over the joystick to set the angles of the stiffness ellipsoid, thus the participants generally did not agree with S2. The participants agreed with S3 and perceived the mental workload to be higher for Mode 1 compared to Mode 2. The participants were generally neutral regarding S4 and the physical workload was perceived to be similar between Mode 1 and Mode 2.

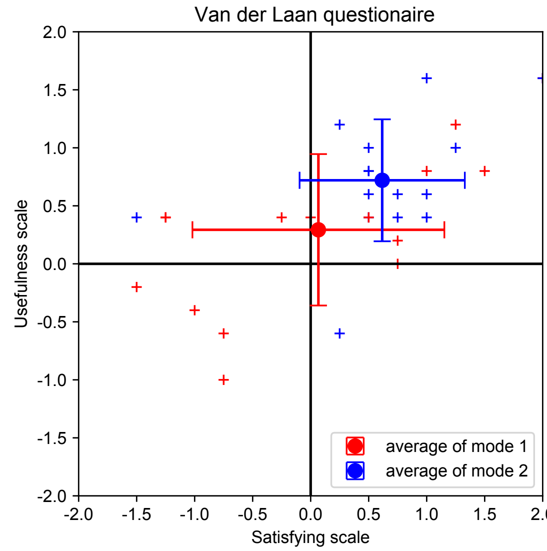

Fig. 8: Results of the van der Laan questionnaire for the acceptance scale. The x-axis is the perceived satisfaction scale, while the y-axis is the perceived usefulness. Markers positioned at the right and at the top sub-planes indicate a higher perception of satisfaction and usefulness, respectively. Mean scores are shown by the dots surrounded by the lines that indicate standard deviation. Individual participant's scores are indicated by the + symbols.

Results of the van der Laan questionnaire are displayed in Fig. 8. Values on the right side of the y-axis represent higher perceived satisfaction with the interface mode, while the values above the x-axis represent higher perceived utility. On average, the participants perceived Mode 2 as more useful and satisfying than Mode 1. The mean satisfaction score for Mode 2 was 0.62$\pm$0.71 and for Mode 1 was 0.07$\pm$1.09. Nevertheless, the difference was statistically not significant ($p = 0.11$). The mean usefulness score for Mode 2 was 0.72$\pm$0.52 and for Mode 1 was 0.29$\pm$0.65. However, the difference was also not statistically significant ($p = 0.05$).

B. Experiment 2: Demonstration

Based on the results of the first experiments, Mode 2 performed better than Mode 1, and thus was selected for the demonstration experiment. The setup in the second experiment (Fig. 3) employed a teleimpedance system composed of the developed stiffness command interface for stiffness control, Force Dimension Sigma7 haptic device for position control, and KUKA LBR iiwa7 robotic arm as a remote robot. The task involved inserting a peg held by the remote robot end-effector and then moving it inside a tight U-shaped slot with an upward ramp in the final section. This required 3D adjustments of the stiffness ellipsoid while moving in different sections of the task. One expert teleoperator was used for this demonstration.

The results of the second experiment are shown in Fig. 9. The tasks started with the insertion of a peg into the hole (see the photo on the top left). This required the operator to configure the stiffness ellipsoid to have a prolate shape and be oriented with the hole (see the bottom two graphs). This way, the peg can be easily pushed in the direction of

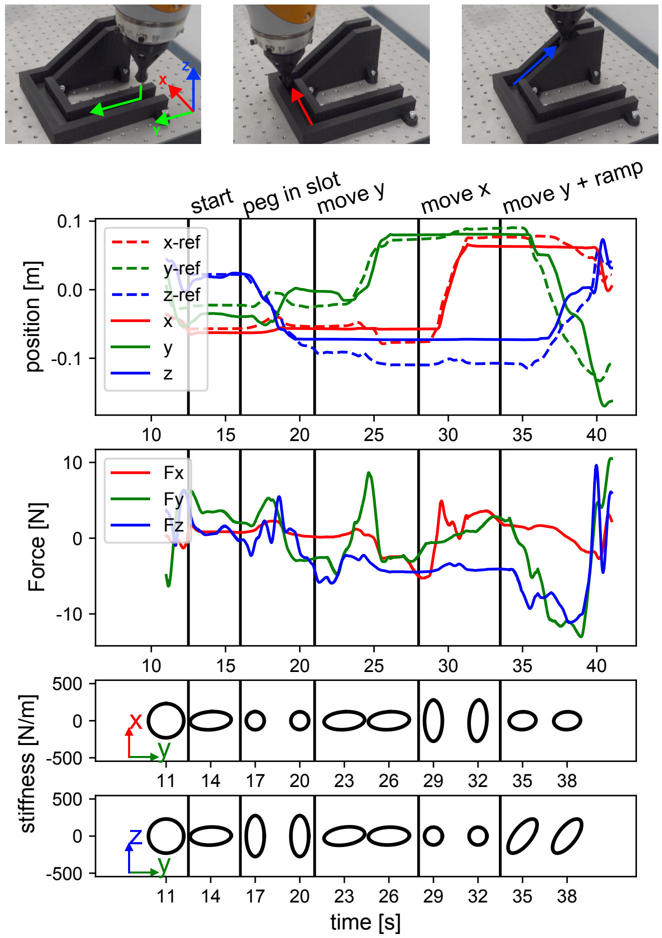

Fig. 9: Results of the second experiment to demonstrate the teleimpedance system with the proposed stiffness command interface on peg-in-the-hole and slide-in-the-slot tasks. The three images on top show the required direction of movement in the key phases of the task. The top graph shows the commanded (dashed lines) and the actual position (solid lines) of the robot end-effector. The second graph displays the interaction forces. The third and fourth graphs depict the stiffness ellipsoid configuration in the x-y and z-y planes.

insertion, while low resistance in the direction perpendicular to insertion makes the peg slide into it smoothly. The insertion is visible by the change in the z-axis position on the top graph. Next, the operator had to align the high-stiffness part of the ellipsoid with the direction of the slot to have the power to move, while the directions toward the walls were set to low stiffness to comply with the environment and minimize friction. The movement along the slot is visible by the change in the y-axis position on the top graph. When reaching the first corner, the operator changed the stiffness configuration to be aligned with the slot in the x-axis, before moving it (see the photo in the top middle). Finally, when the second corner was reached, the operator adjusted the stiffness configuration to be aligned diagonally on the y-z plane in order to account for the upward ramp, before moving it (see the photo on the top right).

IV. Discussion

Using the proposed teleimpedance interface, the operator can adjust the robot's 3D impedance configuration depending on the task requirements during real-time teleoperation. The interface can be easily and quickly equipped and does not require time-consuming calibration procedures. The functionality of the impedance command interface was successfully tested with the virtual impedance alignment tasks, using two different interface configurations and a 3D test environment during teleoperation.

Several observations can be made concerning the completion time. From the results in Fig. 4, we cannot draw a clear conclusion about which mode is better regarding the total task completion times. While no significant difference was observed in the total task completion time, there is a statistically significant difference in the angle alignment time (Fig. 5) and shape/size adjustment time (Fig. 6). This difference is in favour of scroll-wheel inputs compared to joystick input. Similarly, this difference is in line with subjective perception revealed by the results of the Likert questionnaire (Fig. 5).

These results indicate that the 0th-order inputs may be more suitable for adjusting the orientation and shape/size of stiffness ellipsoids, compared to 1st-order inputs. However, the downside of 0th-order inputs like a scroll wheel is that they may have mechanical limits due to encoders. On the other hand, 1st-order inputs such as a joystick are not affected by such mechanical limits since the controlled value is based on the integration of the input. Nevertheless, with 1st-order inputs, we need to consider a trade-off related to the speed of integration. If it is too fast, it is hard to make fine adjustments to the controlled value. If it is too slow, the task performance may suffer.

With both interface modes employing 0th-order and 1st-order input methods, the participants preferred control Mode 2 over Mode 1. Looking closely at the scores of individual participants from the van der Laan questionnaire (Fig 8), the participants had polarising opinions on Mode 1. One group gave Mode 1 nearly the same high usefulness and satisfying scores as Mode 2, while the other perceived it as less satisfying and less useful.

A comparison between the proposed new interface and state-of-the-art interfaces can be made through the results of the van der Laan questionnaire. The van der Laan questionnaire is standardised and acts as an absolute metric, which was also used in the previous study [23] with a very similar experiment to evaluate push-button and touchscreen interfaces. The van der Laan results for the push button were perceived to be slightly less useful and satisfactory than the touchscreen interface. The results here indicate that Mode 2 was perceived as slightly better than the touchscreen interface, while Mode 1 was perceived as slightly worse than the push-button interface. Nevertheless, further studies are needed to provide more insights.

In our experiment, the participants adjusted a single value at a time, even though the interface enables simultaneous control. With extended training and experience, the participants could potentially learn to adjust multiple values simultaneously, which could reduce the task completion times. Several participants also commented that they expected or preferred some interface inputs to work differently. For example, reversing the input directions for increasing and decreasing the controlled value. These observations highlight the importance of personalised training and functionality tailoring of interfaces.

Since the proposed interface does not rely on measuring physiological signals (e.g., EMG), there is no coupling effect between the force feedback and the commanded stiffness [14]. This means that force feedback does not interrupt the stiffness commands generated by the operator, which is advantageous in most cases. However, this also means that any potentially beneficial traits of fast involuntary reflexes cannot be exploited. This trade-off has to be considered when applying this interface to specific tasks.

In the experiment in this study, the teleoperation involved the control of a single remote robotic arm, thus the operator could hold the proposed teleimpedance interface in one hand while the haptic device was in the other arm. When dual-arm teleoperation is needed, the interface could be attached to the end-effector of the haptic device. This way two teleimpedance interfaces in combination with two haptic devices could be used so that each pair can control the stiffness and motion of each remote robot.

A potential future work direction is to redesign the interface to include four scroll wheels (four 0th-order inputs), instead of two scroll wheels (two 0th-order inputs) and a joystick (two 1st-order inputs). Based on the results of this study, a combination of 0th-order inputs could yield an interface with better total task completion times. As a rough estimate, if we hypothetically take the mean angle completion time of Mode 1 (6.85 seconds) and the mean shape/size completion time of Mode 2 (11.07 seconds) that were controlled by the 0th-order inputs, the total competition time would amount to 17.92 seconds. Thus, this hypothetical completion time would be significantly faster compared to the 23 seconds and 22 seconds of Mode 1 and Mode 2, respectively. However, the actual result would probably differ as operating two additional scroll wheels instead of a joystick adds complexity and may affect ergonomics and perceived usability/satisfaction. Therefore, further human factors studies are needed in the future.

References

[1] K. Kaneko, M. Morisawa, S. Kajita, S. Nakaoka, T. Sakaguchi, R. Cisneros, and F. Kanehiro, "Humanoid robot HRP-2Kai–improvement of HRP-2 towards disaster response tasks," in *2015 IEEE-RAS 15th International Conference on Humanoid Robots (Humanoids)*, 2015, pp. 132–139.

[2] K. Darvish, L. Penco, J. Ramos, R. Cisneros, J. Pratt, E. Yoshida, S. Ivaldi, and D. Pucci, "Teleoperation of humanoid robots: A survey," *IEEE Transactions on Robotics*, vol. 39, no. 3, pp. 1706–1727, 2023.

[3] W. Si, N. Wang, and C. Yang, "A review on manipulation skill acquisition through teleoperation-based learning from demonstration," *Cognitive Computation and Systems*, vol. 3, no. 1, pp. 1–16, 2021.

[4] M. Suomalainen, Y. Karayiannidis, and V. Kyrki, "A survey of robot manipulation in contact," *Robotics and Autonomous Systems*, vol. 156, p. 104224, 2022.

[5] A. Naceri, T. Schumacher, Q. Li, S. Calinon, and H. Ritter, "Learning optimal impedance control during complex 3d arm movements," *IEEE Robotics and Automation Letters*, vol. 6, no. 2, pp. 1248–1255, 2021.

[6] F. J. Abu-Dakka and M. Saveriano, "Variable impedance control and learninga review," *Frontiers in Robotics and AI*, vol. 7, p. 590681, 2020.

[7] L. Peternel and A. Ajoudani, "After a decade of teleimpedance: A survey," *IEEE Transactions on Human-Machine Systems*, vol. 53, no. 2, pp. 401–416, 2022.

[8] A. Ajoudani, C. Fang, N. Tsagarakis, and A. Bicchi, "Reduced-complexity representation of the human arm active endpoint stiffness for supervisory control of remote manipulation," *The International Journal of Robotics Research*, vol. 37, no. 1, pp. 155–167, 2018.

[9] S. Park, W. Lee, W. K. Chung, and K. Kim, "Programming by demonstration using the teleimpedance control scheme: Verification by an semg-controlled ball-trapping robot," *IEEE Transactions on Industrial Informatics*, vol. 15, no. 2, pp. 998–1006, 2018.

[10] C. Yang, C. Zeng, C. Fang, W. He, and Z. Li, "A dmps-based framework for robot learning and generalization of humanlike variable impedance skills," *IEEE/ASME Transactions on Mechatronics*, vol. 23, no. 3, pp. 1193–1203, 2018.

[11] J. Li, G. Li, Z. Chen, and J. Li, "A novel emg-based variable impedance control method for a tele-operation system under an unstructured environment," *IEEE Access*, vol. 10, pp. 89 509–89 518, 2022.

[12] E. Hocaoglu and V. Patoglu, "semg-based natural control interface for a variable stiffness transradial hand prosthesis," *Frontiers in Neurorobotics*, vol. 16, p. 789341, 2022.

[13] S. Buscaglione, N. L. Tagliamonte, G. Ticchiarelli, G. Di Pino, D. Formica, and A. Noccaro, "Tele-impedance control approach using wearable sensors," in *2022 44th Annual International Conference of the IEEE Engineering in Medicine & Biology Society (EMBC)*. IEEE, 2022, pp. 2870–2873.

[14] L. M. Doornebosch, D. A. Abbink, and L. Peternel, "Analysis of coupling effect in human-commanded stiffness during bilateral tele-impedance," *IEEE Transactions on Robotics*, vol. 37, no. 4, pp. 1282–1297, 2021.

[15] H. Ahn, Y. Michel, T. Eiband, and D. Lee, "Vision-based approximate estimation of muscle activation patterns for tele-impedance," *IEEE Robotics and Automation Letters*, vol. 8, no. 8, pp. 5220–5227, 2023.

[16] D. S. Walker, R. P. Wilson, and G. Niemeyer, "User-controlled variable impedance teleoperation," in *2010 IEEE International Conference on Robotics and Automation (ICRA)*, 2010, pp. 5352–5357.

[17] L. Peternel, T. Petrič, and J. Babič, "Robotic assembly solution by human-in-the-loop teaching method based on real-time stiffness modulation," *Autonomous Robots*, vol. 42, no. 1, pp. 1–17, 2018.

[18] V. R. Garate, S. Gholami, and A. Ajoudani, "A scalable framework for multi-robot tele-impedance control," *IEEE Transactions on Robotics*, vol. 37, no. 6, pp. 2052–2066, 2021.

[19] A. Giammarino, J. M. Gandarias, and A. Ajoudani, "An open tele-impedance framework to generate data for contact-rich tasks in robotic manipulation," in *2023 IEEE International Conference on Advanced Robotics and Its Social Impacts (ARSO)*. IEEE, 2023, pp. 140–146.

[20] S. Klevering, W. Mugge, D. A. Abbink, and L. Peternel, "Foot-operated tele-impedance interface for robot manipulation tasks in interaction with unpredictable environments," in *2022 IEEE/RSJ International Conference on Intelligent Robots and Systems (IROS)*, 2022, pp. 3497–3504.

[21] J. Schol, J. Hofland, C. J. Heemskerk, D. A. Abbink, and L. Peternel, "Design and evaluation of haptic interface wiggling method for remote commanding of variable stiffness profiles," in *2021 20th International Conference on Advanced Robotics (ICAR)*, 2021, pp. 172–179.

[22] G. Gourmelen, B. Navarro, A. Cherubini, and G. Ganesh, "Human guided trajectory and impedance adaptation for tele-operated physical assistance," in *2021 IEEE/RSJ International Conference on Intelligent Robots and Systems (IROS)*, 2021, pp. 9276–9282.

[23] L. Peternel, N. Beckers, and D. A. Abbink, "Independently commanding size, shape and orientation of robot endpoint stiffness in tele-impedance by virtual ellipsoid interface," in *2021 20th International Conference on Advanced Robotics (ICAR)*, 2021, pp. 99–106.

[24] A. Albu-Schaffer, C. Ott, U. Frese, and G. Hirzinger, "Cartesian impedance control of redundant robots: Recent results with the dlr-light-weight-arms," in *2003 IEEE International Conference on Robotics and Automation (ICRA)*, vol. 3, 2003, pp. 3704–3709.

[25] J. D. Van Der Laan, A. Heino, and D. De Waard, "A simple procedure for the assessment of acceptance of advanced transport telematics," *Transportation Research Part C: Emerging Technologies*, vol. 5, no. 1, pp. 1–10, 1997.